Electronic Supplementary Material

Materials and Methods

Data

Sources of Museum Specimens. Primary distributional data were derived from the collections of the Academy of Natural Sciences (Philadelphia), American Museum of Natural History (New York), Carnegie Museum of Natural History (Pittsburgh), Colección Ornitológica Phelps (Caracas), Delaware Museum of Natural History, Field Museum of Natural History (Chicago), L'Institute Royal des Sciences Naturelles (Bruxelles), Louisiana State University Museum of Natural Sciences, Moore Laboratory of Zoology (Los Angeles), Museo Argentino de Ciencias Naturales (Buenos Aires), Museo de Historia Natural "Javier Prado" de la UNMSM (Lima), Museo de Historia Natural Universidad de Cauca (Popayán), Museo Ecuatoriano de Ciencias Naturales, (Quito), Museo Nacional de Ciencias Naturales (Bogotá), Museo Nacional de Historia Natural (La Paz), Museo Nacional de Historia Natural (Santiago), Museu de Zoologia da Universidade de São Paulo, Museu Nacional (Rio de Janeiro), Museu Paraense Emílio Goeldi (Belém), Museum Alexander Humboldt (Berlin), Museum Alexander Köenig (Bonn), Museum of Comparative Zoology(Harvard University), Museum of Natural History of Los Angeles County, Muséum d'Historie Naturelle (Neuchatel), Muséum National d'Histoire Naturelle (Paris), National Museum of Natural History (Washington, D.C.), Natural History Museum of Gothenburgh, Rijksmuseum van Natuurlijke Historie (Leiden), Royal Ontario Museum (Toronto), Swedish Museum of Natural History (Stockholm), The Natural History Museum (London and Tring), Western Foundation of Vertebrate Zoology (Los Angeles), Zoological Museum (University of Copenhagen).

Models

The two basic models (the Range Scatter model and the Range Cohesion model) are described in general terms in the body of this article. Here we note additional details.

Range Size Frequencies Distributions. The observed number of grid cells occupied by each species was preserved in all stochastic models, so that the modelled range size frequency distribution (RSFD) always matched the observed RSFD, and the modelled richness map matched the observed richness map in terms of the grand total number of *cell x species* occurrences. Using the empirical RSFD in species richness models preserves the direct effect of environmental factors (including gradients, seasonality, and adaptive limits) on the statistical distribution of range size, while not directly determining range placement or richness (Colwell *et al.* 2005), ensuring that model results depend on patterns of range placement, not on the departure of a theoretical model for the RSFD from the observed RSFD (Colwell *et al.* 2004).

Map Cell Probabilities. For each of the ten environmental drivers modelled (table 1, main text, as detailed above), we prepared a *probability map*, represented mathematically as a rectangular matrix composed of 90 rows and 80 columns, with each cell representing a 1° x 1° latitude-longitude region of the map of South America and its surroundings. The

1,676 terrestrial cells (including inland lakes and rivers), arranged in their correct geographic relationship to one another, were each assigned a non-zero probability of occurrence, as specified below. These terrestrial cells represent the bounded geographical *domain* for the stochastic models. (Occurrence probability was set to zero in the remaining 5524 cells, which represented the Atlantic and Pacific oceans, the Gulf of Mexico, and portions of eastern Panama.)

To create the probability map for a particular environmental variable x, we began with raw value x_{ij} for cell in row i, column j of the matrix (terrestrial cells only). Maps of these raw values for most of the environmental drivers are illustrated in figure 1 (main text). (Surface area is not illustrated, and the raw values for the geometric constraints model are uniform.) The raw probability of occurrence P_{ij} for the cell was then defined as

$$P_{ij} = \frac{x_{ij}}{\sum_i \sum_j x_{ij}}, \quad \sum_i \sum_j P_{ij} = \tilde{1} \qquad \text{Equation 1}$$

For the simple environmental variables, Equation 1 assumes the probability of species occurrence is proportional to the magnitude of environmental factor. Under this assumption, if ranges are small compared to the size of the domain (as for the avifauna of South America), the relationship between the environmental factor and expected species richness is also approximately linear, with no intermediate peak of richness. We did not find evidence of strong non-linearities in avian species richness as a function of environmental variables. Supplementary Fig. 1 illustrates one of these patterns by means of simple, bivariate scatterplots of observed species richness as a function of NPP in each grid cell. At the spatial scale of our analyses, there appears to be little non-linearity in these relationships, supporting our use of probability maps (P_{ij}) based on linear scaling of the simple environmental variables (x_{ij}) (Equations 1 and 2).

For the Range Scatter model and, separately, for the Range Cohesion model, ranges were placed stochastically in an initially empty, 90 row by 80 column species *richness map*, guided by each of the ten environmental probability maps. Thus there were 20 models in all. For a given model, all species' ranges were assigned to a richness map stochastically, using the same environmental probability map. The distribution of each species was mapped as a matrix of ones (present in cell) and zeros (absent from cell). The total species richness for each cell was equal to the sum of species occurrences.

Initial Occurrence. The initial cell chosen for each species was chosen stochastically, based on the environmental probability maps. Mathematically, the probability that the initial occurrence for a species' range was in cell (i, j) was simply P_{ij} (Equation 1, above). Thus, initial occurrence was more likely in some grid cells than others, based on their environmental characteristics. The procedure for assigning the cell of initial occurrence was identical for the Range Scatter and Range Cohesion and models. The models differed only in how subsequent cells were chosen.

Subsequent Events. In the Range Cohesion model (based on the "spreading dye" model of Jetz & Rahbek 2001), the placement of each range was completed by choosing any second and subsequent cells from among the set of terrestrial cells bordering (by sides of corners) the cells already occupied by that species, with the choice again guided probabilistically by the values of the environmental probability map in those cells.

Mathematically, if there were N terrestrial cells bordering the cell or cells already occupied by the species, but not yet occupied by the species, the probability Q_{ij} of cell (i, j) being chosen from among the N was

$$Q_{ij} = \frac{P_{ij}}{\sum_i \sum_j P_{ij}}, \quad \sum_i \sum_j Q_{ij} = 1, \qquad\qquad \text{Equation 2}$$

where the summations were taken over the N candidate cells. The probability of any other cell being chosen was zero. With this algorithm, range cohesion was enforced, but the initial placement and the subsequent assignment of occurrences that locate and shape the range were guided by the environmental probability map.

In contrast, the Range Scatter model enforced no range cohesion. Second and subsequent cells were chosen from among all terrestrial cells not already occupied by that species, anywhere in the richness map, whether or not adjacent to cells already occupied by the species, guided by the cell values of the environmental probability map. Mathematically, if there were N terrestrial cells on the entire map that were not yet occupied by the species, then the probability of cell (i, j) being chosen, at any given step of the process, is exactly as in the Equation 2 above, with the summations take over all N candidate cells.

Our models assumed complete independence among species, so the presence of one species did not affect the probability of occurrence of any other species. Once all species occurrences were placed, the species richness for each cell was summed and recorded. The stochastic range placement procedure was repeated 300 times for each of the 10 environmental maps and for the Range Scatter and Range Cohesion models (20 set of runs in all), as listed in Table 1 (main text). Each iteration of the procedure was initiated by setting the random number seed from the system clock. At the conclusion of each set of 300 iterations a particular model, the average number of species recorded in each map cell was taken to be the statistical expectation of richness per cell for that model. Because modelled cell richness for each run is the sum of many independent, stochastic processes of range placement (one for each species), the distribution of modelled cell values, among runs, converges on a normal distribution by the central limit theorem. Approximate normality has been demonstrated for one-dimensional models based on the corresponding range placement algorithm (R. Colwell, unpublished data). The analyses were conducted with a dedicated software application built by Gary Entsminger in Delphi 7.0 and run on a Windows PC.

The assumption of range cohesion. In a heterogeneous environment, the Range Cohesion model integrates the simple, but often realistic geometric constraints that produce the mid-domain effect (boundary constraints and range cohesion (Colwell *et al.* 2004) with environmental heterogeneity. The result is a unified, stochastic model that incorporates a further element of realism by weighting the probability of occurrence in map cells by an environmental factor or factors. However, the qualitative results of this model do not require an assumption of strict range cohesion. Stochastic models based on a Poisson dispersal function from occupied cells produce qualitatively similar results for small or moderate dispersal distances (see also Connolly 2005). At large dispersal distances, this Poisson model converges to the Range Scatter model (Gotelli *et al.,* unpublished results).

Statistical Analyses. Each of the 95 stochastic models (main text, table 1) generated an expected species richness value for every $1 \times 1°$ grid cell in the map. We compared the quantitative fit of observed species richness to these model predictions for each model. All statistical analyses of observed and predicted species richness were conducted in the dedicated software package Spatial Analysis in Macroecology (SAM, Version 1.1; Rangel *et al.* 2006).

We did not produce predicted richness maps for the five Range Scatter models for environmentally homogeneous maps (indicated by *n/a* in Table 1 in the main text), because the results would themselves be stochastically uniform.

As an initial assessment of the remaining 95 stochastic models, we fit the observed species richness to the expected species richness using an ordinary least-square (OLS) regression model (Sokal & Rohlf 1995). However, because the analysis is based on gridded data, pairs of observations at a given spatial distance may be not statistically independent, and this spatial autocorrelation may inflate Type I errors in statistical analysis (Legendre 1993; Diniz-Filho *et al.* 2003). To quantify the amount of spatial autocorrelation contaminating the OLS regression model, we analyzed spatial autocorrelation in regression residuals using Moran's *I* coefficient

$$I(d) = \left(\frac{n}{S}\right) \frac{\sum_{j=1}^{n}\sum_{i=1}^{n} w_{ji}(y_j - \bar{y})(y_i - \bar{y})}{\sum_{i=1}^{n}(y_i - \bar{y})^2}, \text{ for } j \neq i$$

where *d* indexes the different distance classes, y_i and y_j are observations measured at sites *i* and *j*, $\bar{y}$ is the grand mean, *n* is the total number of sampling sites, and *S* is number of pairs of observations (or their weights) for a given distance class (Legendre & Legendre 1998). For this analysis, we used geodesic surface distances, which take into account the earth's curvature.

We used a standardized measure of spatial autocorrelation (de Jong *et al.* 1984; Lichstein *et al.* 2002), the ratio of Moran's I to its maximum possible value $I(d)/I_{max}(d)$, where $I_{max}(d)$ is defined as

$$\left|I_{max}(d)\right| = \frac{n}{S}\left\{\sum_{i=1}^{n}\left[\sum_{j=1}^{n} w_{ij}(y_j - \bar{y})\right]^2 / \sum_{i=1}^{n}(y_i - \bar{y})\right\}^{1/2}, \text{ for } j \neq i,$$

and w_{ij} is the geographic distance between sampling sites *i* and *j*.

We calculated $I(d)/I_{max}(d)$ for spatial distance *d* ranging between 0 and 500 km, and considered as spatially autocorrelated those residuals with $I(d)/I_{max}(d)$ higher than 0.3. According to this criterion, all our OLS models were spatially autocorrelated. Note that this is a conservative criterion that may over-estimate the importance of spatial autocorrelation because it is based on a standardized Moran's *I* calculated over a relatively short distance of 500 km (where positive autocorrelation is most likely to occur).

Next, we calculated the effective number of degrees of freedom (*n**) according to Dutilleul's method (Dutilleul 1993; Dale *et al.* 2002):

$$n* = 1 + n^2 \left[\text{trace} \left(\hat{\mathbf{R}}_{Y1} \hat{\mathbf{R}}_{Y2} \right) \right]^1$$

where $\hat{\mathbf{R}}$ are square matrices (n x n) describing the spatial correlation of the variables $\mathbf{Y}_1$ and $\mathbf{Y}_2$, built using the spatial correlograms of these variables, and n is total number of sampling sites. This method reduces the number of degrees of freedom in a linear correlation analysis according to the magnitude of spatial autocorrelation in both variables, as measured by a correlogram. The significance of r^2 (or, equivalently, of the test for a slope of 0.0) in an OLS regression can be evaluated in the presence of spatial autocorrelation using $n*$, which corrects for the inflation of Type I error due to autocorrelation. Without this adjustment, the sample size in our analyses is so large (n =1676 grid cells) that patterns would be statistically significant at $P = 0.05$ for any $r^2 > 0.005$.

Because the OLS residuals were spatially autocorrelated in all of our models, we used a generalized least squares (GLS, sometimes called "kriging regression" Haining 1990; Cressie 1993) model to estimate the "true" regression coefficients (β), while taking the spatial component into account:

$$\beta = \left(\mathbf{X}^T \mathbf{C}^{-1} \mathbf{X} \right)^{-1} \mathbf{X}^T \mathbf{C}^{-1} \mathbf{Y}$$

where $\mathbf{Y}$ is the response variable (observed species richness), $\mathbf{X}$ is the explanatory variable (predicted species richness from a particular stochastic model), and $\mathbf{C}$ is a square matrix (n x n) describing the covariance among pairs of OLS residual values (Haining 1990; Cressie 1993). For each model, the matrix $\mathbf{C}$ was modelled by choosing the best fit among the following models describing the semi-variogram of the OLS residuals (Legendre & Legendre 1998; Banerjee *et al.* 2004).

The spherical models are defined as

$$\gamma(d) = C_0 + C_1 \left[1.5 \frac{d}{a} - 0.5 \left(\frac{d}{a} \right)^3 \right] \text{ if } d \leq a$$

$$\gamma(d) = C_0 + C_1 \text{ if } d > a$$

$$\text{cov}(d) = 0 \text{ if } d \geq 0$$

$$\text{cov}(d) = C_1 \left[1 - 1.5 \frac{d}{a} + 0.5 \left(\frac{d}{a} \right)^3 \right] \text{ if } 0\, d \leq 1$$

$$\text{cov}(d) = C_0 + C_1 \text{ otherwise}$$

The exponential models are defined as

$$\gamma(d) = C_0 + C_1 \left[1.5 - \exp \left(-3 \frac{d}{a} \right) \right]$$

$$\text{cov}(d) = C_1 \left[\exp \left(-3 \frac{d}{a} \right) \right]$$

The Gaussian models are defined as

$$\gamma(d) = C_0 + C_1 \left[1 - \exp \left(-3 \frac{d^2}{a^2} \right) \right]$$

$$\text{cov}(d) = C_1 \left[\exp \left(-3 \frac{d^2}{a^2} \right) \right]$$

The hole effect, or wave, models are defined as

$$\gamma(d) = C_0 + C_1\left[1 - \frac{\sin(ad)}{ad}\right] \qquad\qquad \text{cov}(d) = C_1\left[\frac{\sin(ad)}{ad}\right] \quad \text{if } a > 0$$

where γ is the semi-variance; *cov* is the covariance; d is the distance among pairs of sampling sites; and C_0, C_1, and a are fitted parameters (Legendre & Legendre 1998).

GLS is a regression in which the spatial component is defined by the fitted semi-variogram and is explicitly modelled in the residual terms. Therefore, these residuals contain a strong spatial component, which must be decomposed using Cholesky decomposition into spatially-structured residuals and a pure error term (Haining 1990; Cressie 1993). This error vector **e**, or noise component, is defined as

$$\mathbf{e} = \mathbf{L}^{-1}(\mathbf{Y} - \mathbf{X}\boldsymbol{\beta})$$

where $\boldsymbol{\beta}$ is the vector of estimated slopes and $\mathbf{LL}^{\mathbf{T}} = \mathbf{C}$, so that the **L** matrix can be obtained by the Cholesky decomposition of the covariance among residuals.

After fitting the GLS model, we calculated $I(d)/I_{\max}(d)$ for spatial distance d ranging between 0 and 500 km of the GLS error term. To determine whether the fitted GLS model effectively controlled for spatial autocorrelation, we assessed the significance of the overall spatial correlogram (using 20 distance classes) using the Bonferroni correction for multiple tests of significance (Diniz-Filho *et al.* 2003). We found that, for all of the correlograms, none of the Moran's *I* coefficients was significant at $P = 0.1$. However, for the error term of 5 GLS models, $I(d)/I_{\max}(d)$ was higher than 0.5 for the distance class 0-500 km. Therefore, for these cases, we fit a Simultaneous Autoregressive Model (SAR, Haining 1990; Cressie 1993), which is a GLS-based model, but with the matrix **C** defined as

$$\mathbf{C} = \sigma^2\left[(\mathbf{I} - \rho\mathbf{W})^T\right]^{-1}\left[(\mathbf{I} - \rho\mathbf{W})\right]^{-1}$$

where σ^2 is the variance of the OLS residuals, ρ is the autoregression parameter to be estimated for the model, **W** is matrix of neighbour weights, computed as an inverse power function of geographic distances among sampling units $\left(w_{ij} = 1/d_{ij}^3\right)$, and **I** is an n x n identity matrix. Among the 5 models that required SAR, $I(d)/I_{\max}(d)$ decreased in 4 models in the distance class 0-500 km, and the overall correlograms remained non-significant.

Model Selection. To choose among competing models for each data quartile, we used the spatially corrected slope values (based on the GLS or SAR models) and the corrected *P* value for the statistical significance of r^2 (based on Dutilleul's method). We used a hierarchical method to determine the best-fitting models. First, we eliminated any model for which the statistical significance of r^2 was $P > 0.05$. For these models, we could not reject the null hypothesis that the relationship between observed and predicted species richness was not different from zero. This criterion eliminated 53 of the 95 models (unshaded cells in table 1, main text, and Supplementary table 1). Next, we eliminated models for which the 95% confidence interval of the spatially corrected slope did not bracket 1.0. The predicted species richness in these models was correlated with observed richness, but the quantitative prediction of a slope of 1.0 was not met (Romdal *et al.*

2005). This criterion eliminated 37 of the remaining 42 models (shaded in gray in table 1, main text, and Supplementary table 1). Thus, of the 95 original models, only 5 models had slopes that were significantly different from 0.0, but whose 95% confidence intervals bracketed 1.0 (shaded in green in table 1 main text, and Supplementary table 1), after accounting for spatial autocorrelation. For Quartile 2 only 1 model fit these criteria. For Quartiles 1 and 3 and for all species, none of the models fit these criteria. For Quartile 4 (the most widespread species), 4 models (Geometric Constraints, Temperature, Water-Energy, and Temperature Kinetics) met these criteria. Of these 4, we eliminated the Geometric Constraints model because its slope (0.74) was substantially shallower than the slopes for theWater-Energy (1.03), Temperature (0.98), and Temperature Kinetics (0.99) models. Among these three models, we chose the Water-Energy model as the best fitting because its r^2 value was slightly higher, and its intercept bracketed zero (Supplementary table 1).

References

Allen, A. P., Brown, J. P. & Gillooly, J. F. 2002. Global biodiversity, biochemical kinetics, and the energetic-equivalence rule. *Science* **297**, 1545-1548.

Allen, A. P., Gillooly, J. F., Savage, V. M. & Brown, J. H. 2006. Kinetic effects of temperature on rates of genetic divergence and speciation.

Banerjee, S. Carlin, B.P. & Gelfand, A.E.2004. *Hierarchical modeling and analysis for spatial data* Boca Raton, FL: Chapman & Hall.

Brown, J. H., Gillooly, J. F., Allen, A. P., Savage, V. M. & West, G. B. 2004 Toward a metabolic theory of ecology. *Ecology* **85**, 1771-1789.

Colwell, R. K., Rahbek, C. & Gotelli, N. J. 2004. The mid-domain effect and species richness patterns: What have we learned so far? *Am. Nat.* **163**, E1-E23.

Colwell, R. K., Rahbek, C. & Gotelli, N. J. 2005 The mid-domain effect: There's a baby in the bathwater *American Naturalist* **166**, E149–E154.

Connolly, S. R. 2005. Process-based models of species distributions and the mid-domain effect. *American Naturalist* **166**, 1-11.

Cressie, N. A. C. *Statistics for Spatial Data* (Wiley, New York, 1993).

Currie, D. J., Mittlebach, G. G., Cornell, H. V., Field, R., Guegan, J., Hawkins, B. A., Kaufman, D. M., Kerr, J. T., Oberdoff, T., O'Brien, E. & Turner, J. P. G. 2004 Predictions and tests of climate-based hypotheses of broad-scale variation in taxonomic richness. *Ecol. Lett.* **7**, 1121-1134.

Dale, M. R. T., P. Dixon, M. J. Fortin, P. Legendre, D. E. Myers, and M. S. Rosenberg. 2002. Conceptual and mathematical relationships among methods for spatial analysis. Ecography 25:558 – 577.

de Jong, P., Sprenger, C. & van Veen, F. 1984 On extreme values of Morans-I and Gearys-C. *Geograph. Anal.* **16**, 17-24.

Diniz-Filho, J. A. F., Bini, L. M. & Hawkins, B. A. 2003 Spatial autocorrelation and red herrings in geographical ecology *Glob. Ecol. Biogeog.* **12**, 53-64.

Dutilleul, P. 1993 Modifying the t-test for assessing the correlation between 2 spatial processes. *Biometrics* **49**, 305-314.

Gotelli, N. J. & Colwell, R. K. 2001 Quantifying biodiversity: procedures and pitfalls in the measurement and comparison of species richness *Ecol. Lett.* **4**, 379-391.

Haining, R. 1990 *Spatial data analysis in the social and environmental sciences* Cambridge, UK: Cambridge Univ. Press.

Hawkins, B. A., Field, R., Cornell, H. V., Currie, D. J., Guegan, J. F., Kaufman, D. M., Kerr, J. T., Mittlebach, G. G., Oberdoff, T., O'Brien, E. M., Porter, E. E. & Turner, J. R. G. 2003 Energy, water, and broad-scale geographic patterns of species richness. *Ecology* **84**, 3105-3117.

Jennes, J. 2002 *Surface areas and ratios from elevation grid (surgrids.avx) extension for ArcView 3.x, v. 1.2.* (available at http://www.jennessent.com/arcview/surface_areas.htm).

Jetz, W. & Rahbek, C. 2001 Geometric constraints explain much of the species richness pattern in African birds. *Proc. Natl. Acad. Sci. USA* **98**, 5661-5666.

Jetz, W. & Rahbek, C. 2002. Geographic range size and determinants of avian species richness. *Science* **297**, 1548-1551.

Legendre, P. & Legendre, L. 1998 *Numerical Ecology* New York, NY: Elsevier.

Legendre, P. Spatial autocorrelation – trouble or new paradigm 1993 *Ecology* **74**, 1659-1673.

Lichstein, J. W., Simons, T. R., Shriner, S. A. & Franzreb, K. E., 2002 Spatial autocorrelation and autoregressive models in ecology. *Ecol. Monog.* **72**, 445-463.

New M., Hulme, M. & Jones, P. 1999 Representing twentieth-century space-time climate variability. Part I: Development of a 1961-90 mean monthly terrestrial climatology *J. Climate* **12**, 829-856.

Rahbek, C. & Graves, G. R. 2000. Detection of macro-ecological patterns in South American hummingbirds is affected by spatial scale. *Proc. R. Soc. London Ser. B* **267**, 2259-2265.

Rahbek, C. & Graves, G. R. 2001 Multiscale assessment of patterns of avian species richness. *Proc. Natl. Acad. Sci. USA* **98**, 4534-4539.

Rangel, T. F. L. V. B. J. A. F. Diniz-Filho, and L. M. Bini. 2006. Towards an integrated computational tool for spatial analysis in macroecology and biogeography. Global Ecology and Biogeography 15:321-327

Romdal, T. S., Colwell, R. K. & Rahbek, C. 2005. The influence of band sum area, domain extent, and range sizes on the latitudinal mid-domain effect *Ecology* **86**, 235-244.

Sokal, R. R. & Rohlf, F. J. *Biometry* (Freeman, New York, 1995).

Williams, P. H. 1996 *WORLDMAP 4 WINDOWS: Software and Help Document 4.19* (privately distributed and available at http://www.nhm.ac.uk/science/projects/worldmap).

Woodward, F. I., Smith, T. M. & Emmanuel, W. R. 1995 A global land primary productivity and phytogeography model *Global Biogeochem. Cycles* **9**, 471-490.

Supplementary Information

Supplementary Figure 1

Supplementary Fig. 1. Species richness of South American endemic birds in 1° x 1° (latitude-longitude) cells as a function of net primary productivity (NPP), for first (smallest ranges) through fourth (largest ranges) range size quartiles and for all quartiles combined. Red lines fitted by LOWESS smoothing procedure.
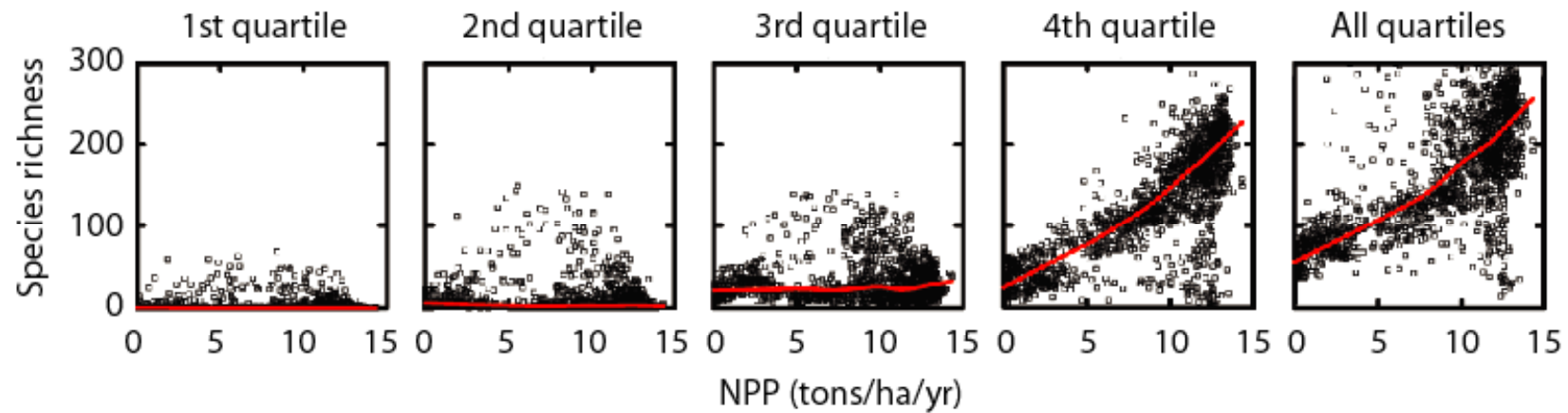
Supplementary Information

Supplementary Tables 1 to 4

Supplementary Table 1. Detailed results from 95 explanatory models for species richness of endemic birds of South America ($n =$ 2,248). (See table 1, main text, for summary results, especially for easier comparison of Range Scatter and Range Cohesion models.) Each titled sub-table (Supplementary Table 1a to 1j), below, represents a range size quartile category (First, Second, Third, Fourth, or All Quartiles) for either Range Scatter or Range Cohesion models. Columns represent environmental models and rows organize the statistical results. A successful model should explain a significant proportion of the variation in species richness and have a slope that is close to 1.0. Unshaded cells indicate non-explanatory models, for which the r^2 value does not differ significantly from 0, based on the effective number of degrees of freedom using Dutilleul's method to adjust for spatial autocorrelation (Dutilleul 1993). Grey cells indicate models for which the r^2 value was significantly different from 0, but for which the 95% confidence interval of the slope for the best-fitting spatial model did not bracket 1.0. (Note that some models in this category have negative slopes.) Green cells (which have italic type) indicate models for which both the r^2 and the slope criterion were satisfied. Within each quartile, the model for which the slope is closest to 1.0 is boldfaced, indicating the best-fitting model for that quartile. Note that for some quartiles, a best-fitting model could not be identified that satisfied our criteria. For the 4th quartile species, the slope values for the Water Energy , Temperature, and Temperature Kinetics models were virtually equidistant from 1.0, but the Water-Energy model was marked as the best because it had a slightly higher r^2 and a better-fitting intercept.

	Topographic surface area	NPP	Precipitation	Temperature	Topographic Relief	Ecosystem Diversity	Species Energy	Water Energy	Temperature Kinetics
	Supplementary Table 1a: First Quartile - Range Scatter Models								
Ordinary Regression									
r^2	0.007	0.003	0.000	0.006	0.342	0.212	0.002	0.003	0.009
P (n*)	0.466	0.738	0.859	0.669	0.000	0.000	0.815	0.776	0.558
$I(d)/I_{max}(d)$ (0-500km)	0.689	0.684	0.683	0.688	0.691	0.701	0.683	0.687	0.688
Spatial Regression	Needed	Needed	Needed	Needed	Needed	Needed	Needed	Needed	Needed
Model	GLS	GLS	GLS	GLS	GLS	GLS	GLS	GLS	GLS
Intercept	9.773	12.524	11.561	18.093	-0.199	1.144	10.700	17.412	36.325
P-Value (H$_0$: a = 0)	0.000	0.000	0.000	0.000	0.935	0.637	0.000	0.000	0.000
Lower C.I. (P=0.95)	4.569	6.848	6.240	12.436	-5.011	-3.601	5.049	11.869	28.877
Higher C.I. (P=0.95)	14.977	18.200	16.882	23.750	4.613	5.889	16.351	22.955	43.773
Slope	1.923	-1.508	-0.889	-4.913	1.532	3.013	-0.722	-5.148	-11.892
P-Value (H$_0$: b = 0)	0.000	0.000	0.000	0.000	0.000	0.000	0.000	0.000	0.000
Lower C.I. (P=0.95)	1.360	-1.986	-1.222	-5.693	1.426	2.772	-1.134	-7.108	-14.181
Higher C.I. (P=0.95)	2.486	-1.030	-0.556	-4.133	1.638	3.254	-0.310	-3.188	-9.603
$I(d)/I_{max}(d)$ (0-500km)	0.430	0.402	0.410	0.425	0.471	0.410	0.404	0.407	0.407

	Supplementary Table 1b: First Quartile - Range Cohesion Models									
	Topographic surface area	NPP	Precipitation	Temperature	Topographic Relief	Ecosystem Diversity	Species Energy	Water Energy	Temperature Kinetics	Geometric Constraints
Ordinary Regression										
r^2	0.005	0.007	0.000	0.006	0.328	0.225	0.007	0.003	0.000	0.009
P (n*)	0.519	0.629	0.911	0.664	0.000	0.000	0.628	0.756	0.827	0.000
$I(d)/I_{max}(d)$ (0-500km)	0.687	0.684	0.683	0.686	0.691	0.708	0.683	0.685	0.685	0.687
Spatial Regression	Needed	Needed	Needed	Needed	Needed	Needed	Needed	Needed	Needed	Needed
Model	GLS	GLS	GLS	GLS	GLS	GLS	GLS	GLS	GLS	GLS
Intercept	10.703	11.804	10.902	13.943	0.980	2.531	9.929	13.565	8.392	4.504
P-Value (H$_0$: a = 0)	0.000	0.000	0.000	0.000	0.674	0.283	0.000	0.000	0.004	0.125
Lower C.I. (P=0.95)	5.440	6.075	5.581	8.253	-3.583	-2.085	4.090	7.963	2.694	-1.245
Higher C.I. (P=0.95)	15.966	17.533	16.223	19.633	5.543	7.147	15.768	19.167	14.090	10.253
Slope	1.394	-1.577	-0.826	-3.087	1.398	2.926	-1.149	-3.398	1.535	3.767
P-Value (H$_0$: b = 0)	0.000	0.000	0.000	0.000	0.000	0.000	0.000	0.000	0.011	0.000
Lower C.I. (P=0.95)	0.910	-2.006	-1.142	-3.763	1.298	2.705	-1.516	-4.096	0.349	2.650
Higher C.I. (P=0.95)	1.878	-1.148	-0.510	-2.411	1.498	3.147	-0.782	-2.700	2.721	4.884
$I(d)/I_{max}(d)$ (0-500km)	0.427	0.404	0.407	0.408	0.468	0.421	0.401	0.395	0.420	0.422

	Topographic surface area	NPP	Precipitation	Temperature	Topographic Relief	Ecosystem Diversity	Species Energy	Water Energy	Temperature Kinetics
Supplementary Table 1c: Second Quartile - Range Scatter Models									
Ordinary Regression									
r^2	0.003	0.004	0.001	0.016	0.419	0.217	0.004	0.008	0.017
P (n*)	0.593	0.704	0.842	0.447	0.000	0.000	0.711	0.603	0.435
$I(d)/I_{max}(d)$ (0-500km)	0.703	0.698	0.698	0.703	0.671	0.703	0.696	0.702	0.703
Spatial Regression Needed	Needed	Needed	Needed	Needed	Needed	Needed	Needed	Needed	Needed
Model	GLS	GLS	GLS	GLS	GLS	GLS	GLS	GLS	GLS
Intercept	27.012	37.181	33.003	59.813	4.939	7.883	33.111	56.152	153.701
P-Value (H$_0$: $a = 0$)	0.000	0.000	0.000	0.000	0.270	0.100	0.000	0.000	0.000
Lower C.I. (P=0.95)	16.518	25.801	22.450	47.918	-3.846	-1.513	21.759	44.502	132.972
Higher C.I. (P=0.95)	37.506	48.561	43.556	71.708	13.724	17.279	44.463	67.802	174.430
Slope	1.166	-0.797	-0.300	-3.768	1.099	1.881	-0.385	-3.461	-13.197
P-Value (H$_0$: $b = 0$)	0.000	0.000	0.009	0.000	0.000	0.000	0.004	0.000	0.000
Lower C.I. (P=0.95)	0.809	-1.109	-0.527	-4.262	1.034	1.726	-0.650	-3.969	-15.116
Higher C.I. (P=0.95)	1.523	-0.485	-0.073	-3.274	1.164	2.036	-0.120	-2.953	-11.278
$I(d)/I_{max}(d)$ (0-500km)	0.424	0.399	0.411	0.406	0.393	0.373	0.401	0.400	0.394

	Supplementary Table 1d: Second Quartile - Range Cohesion Models									
	Topographic surface area	NPP	Precipitation	Temperature	Topographic Relief	Ecosystem Diversity	Species Energy	Water Energy	Temperature Kinetics	Geometric Constraints
Ordinary Regression										
r^2	0.000	0.018	0.000	0.032	0.384	*0.193*	0.022	0.022	0.017	0.001
P (n*)	0.836	0.414	0.877	0.254	0.000	*0.000*	0.373	0.362	0.176	0.456
$I(d)/I_{max}(d)$ (0-500km)	0.697	0.695	0.699	0.695	0.678	*0.719*	0.692	0.696	0.685	0.695
Spatial Regression	Needed	Needed	Needed	Needed	Needed	***Needed***	Needed	Needed	Needed	Needed
Model	GLS	GLS	GLS	GLS	GLS	*GLS*	GLS	GLS	GLS	GLS
Intercept	32.337	35.179	32.626	37.806	8.322	*14.378*	29.931	36.437	34.998	26.791
P-Value (H$_0$: $a = 0$)	0.000	0.000	0.000	0.000	0.071	*0.002*	0.000	0.000	0.000	0.000
Lower C.I. (P=0.95)	21.530	23.211	21.683	25.425	-0.698	*5.144*	17.644	24.346	23.395	15.652
Higher C.I. (P=0.95)	43.144	47.147	43.569	50.187	17.342	*23.612*	42.218	48.528	46.601	37.930
Slope	0.547	-1.165	-0.486	-2.066	0.988	*1.800*	-1.013	-2.144	-0.371	0.988
P-Value (H$_0$: $b = 0$)	0.000	0.000	0.000	0.000	0.000	*0.000*	0.000	0.000	0.195	0.000
Lower C.I. (P=0.95)	0.241	-1.430	-0.694	-2.429	0.925	*1.651*	-1.244	-2.522	-0.932	0.437
Higher C.I. (P=0.95)	0.853	-0.900	-0.278	-1.703	1.051	*1.949*	-0.782	-1.766	0.190	1.539
$I(d)/I_{max}(d)$ (0-500km)	0.423	0.388	0.405	0.392	0.418	*0.409*	0.381	0.382	0.411	0.420

	Supplementary Table 1e: Third Quartile - Range Scatter Models								
	Topographic surface area	NPP	Precipitation	Temperature	Topographic Relief	Ecosystem Diversity	Species Energy	Water Energy	Temperature Kinetics
Ordinary Regression									
r^2	0.013	0.005	0.018	0.017	0.219	0.185	0.004	0.003	0.019
P (n*)	0.170	0.621	0.329	0.308	0.000	0.000	0.644	0.659	0.276
$I(d)/I_{max}(d)$ (0-500km)	0.726	0.717	0.713	0.722	0.762	0.732	0.719	0.711	0.722
Spatial Regression Needed	Needed	Needed	Needed	Needed	Needed	Needed	Needed	Needed	Needed
Model	GLS	GLS	GLS	GLS	GLS	GLS	GLS	GLS	GLS
Intercept	10.646	27.564	21.228	68.280	4.460	2.396	20.791	60.343	14.010
P-Value (H$_0$: $a = 0$)	0.023	0.000	0.000	0.000	0.265	0.572	0.000	0.000	0.000
Lower C.I. (P=0.95)	1.454	17.825	11.708	57.657	-3.390	-5.916	11.571	49.412	-13.450
Higher C.I. (P=0.95)	19.838	37.303	30.748	78.903	12.310	10.708	30.011	71.274	41.470
Slope	0.793	-0.122	0.111	-1.521	0.468	0.679	0.205	-1.266	-6.180
P-Value (H$_0$: $b = 0$)	0.000	0.094	0.041	0.000	0.000	0.000	0.000	0.000	0.000
Lower C.I. (P=0.95)	0.654	-0.265	0.005	-1.739	0.441	0.618	0.091	-1.495	-7.050
Higher C.I. (P=0.95)	0.932	0.021	0.217	-1.303	0.495	0.740	0.319	-1.037	-5.310
$I(d)/I_{max}(d)$ (0-500km)	0.400	0.408	0.403	0.432	0.463	0.419	0.407	0.433	0.429

	Supplementary Table 1f: Third Quartile - Range Cohesion Models									
	Topographic surface area	NPP	Precipitation	Temperature	Topographic Relief	Ecosystem Diversity	Species Energy	Water Energy	Temperature Kinetics	Geometric Constraints
Ordinary Regression										
r^2	0.000	0.000	0.006	0.024	0.171	0.107	0.000	0.012	0.016	0.008
P (n*)	0.827	0.967	0.627	0.238	0.000	0.012	0.839	0.438	0.253	0.343
$I(d)/I_{max}(d)$ (0-500km)	0.715	0.717	0.718	0.708	0.743	0.742	0.716	0.711	0.704	0.707
Spatial Regression	Needed	Needed	Needed	Needed	Needed	Needed	Needed	Needed	Needed	Needed
Model	GLS	GLS	GLS	GLS	GLS	GLS	GLS	GLS	GLS	GLS
Intercept	18.650	30.264	24.930	33.296	4.269	8.955	25.928	33.110	17.464	7.363
P-Value (H$_0$: $a = 0$)	0.000	0.000	0.000	0.000	0.291	0.043	0.000	0.000	0.000	0.146
Lower C.I. (P=0.95)	9.820	20.989	15.685	23.968	-3.651	0.298	16.796	23.602	7.537	-2.553
Higher C.I. (P=0.95)	27.480	39.539	34.175	42.624	12.189	17.612	35.060	42.618	27.391	17.279
Slope	0.895	-0.414	0.006	-0.611	0.533	0.748	-0.183	-0.614	0.542	1.184
P-Value (H$_0$: $b = 0$)	0.000	0.000	0.922	0.000	0.000	0.000	0.012	0.000	0.000	0.000
Lower C.I. (P=0.95)	0.726	-0.573	-0.121	-0.819	0.500	0.674	-0.326	-0.847	0.232	0.872
Higher C.I. (P=0.95)	1.064	-0.255	0.133	-0.403	0.566	0.822	-0.040	-0.381	0.852	1.496
$I(d)/I_{max}(d)$ (0-500km)	0.419	0.399	0.411	0.421	0.477	0.431	0.401	0.416	0.411	0.412

	Supplementary Table 1g: Fourth Quartile - Range Scatter Models								
	Topographic surface area	NPP	Precipitation	Temperature	Topographic Relief	Ecosystem Diversity	Species Energy	Water Energy	Temperature Kinetics
Ordinary Regression									
r^2	0.220	0.625	0.494	0.468	0.217	0.000	0.657	0.545	0.474
P (n*)	0.005	0.000	0.004	0.005	0.002	0.999	0.000	0.003	0.006
$I(d)/I_{max}(d)$ (0-500km)	0.822	0.781	0.809	0.813	0.796	0.894	0.736	0.805	0.813
Spatial Regression Needed	Needed	Needed	Needed	Needed	Needed	Needed	Needed	Needed	Needed
Model	GLS	GLS	GLS	GLS	GLS	GLS	GLS	GLS	GLS
Intercept	83.520	-25.791	-6.364	29.784	38.144	53.622	17.675	-4.137	-142.939
P-Value (H$_0$: $a = 0$)	0.000	0.278	0.729	0.048	0.206	0.004	0.253	0.818	0.000
Lower C.I. (P=0.95)	55.245	-72.384	-42.426	0.237	-21.019	17.372	-12.652	-39.397	-195.732
Higher C.I. (P=0.95)	111.795	20.802	29.698	59.331	97.307	89.872	48.002	31.123	-90.146
Slope	0.050	0.581	0.361	0.410	0.043	0.061	0.420	0.566	1.764
P-Value (H$_0$: $b = 0$)	0.014	0.000	0.000	0.000	0.000	0.000	0.000	0.000	0.000
Lower C.I. (P=0.95)	0.011	0.524	0.316	0.330	0.029	0.039	0.379	0.484	1.413
Higher C.I. (P=0.95)	0.089	0.638	0.406	0.490	0.057	0.083	0.461	0.648	2.115
$I(d)/I_{max}(d)$ (0-500km)	0.069	0.342	0.296	0.040	0.217	0.173	0.468	0.093	0.038

	Supplementary Table 1h: Fourth Quartile - Range Cohesion Models									
	Topographic surface area	NPP	Precipitation	Temperature	Topographic Relief	Ecosystem Diversity	Species Energy	Water Energy	Temperature Kinetics	Geometric Constraints
Ordinary Regression										
r^2	0.481	0.737	0.649	*0.684*	0.238	0.106	0.721	***0.710***	0.517	*0.365*
P (n*)	0.009	0.000	0.002	*0.001*	0.011	0.258	0.000	***0.000***	0.006	*0.029*
$I(d)/I_{max}(d)$ (0-500km)	0.806	0.760	0.809	*0.783*	0.833	0.893	0.755	***0.772***	0.833	*0.861*
Spatial Regression	Needed	Needed	Needed	*Needed*	Needed	Needed	Needed	***Needed***	Needed	*Needed*
Model	GLS	GLS	GLS	*GLS*	GLS	GLS	GLS	***GLS***	GLS	*GLS*
Intercept	87.026	16.226	19.046	*7.339*	18.117	58.237	63.461	***5.219***	-26.169	*20.902*
P-Value (H₀: $a = 0$)	0.000	0.069	0.093	*0.038*	0.441	0.033	0.000	***0.128***	0.000	*0.411*
Lower C.I. (P=0.95)	61.017	-1.275	-3.186	*0.408*	-28.012	4.827	58.040	***-1.494***	-39.962	*-28.919*
Higher C.I. (P=0.95)	113.035	33.727	41.278	*14.270*	64.246	111.647	68.882	***11.932***	-12.376	*70.723*
Slope	0.119	0.888	0.877	*0.981*	0.072	0.227	0.383	***1.025***	1.246	*0.744*
P-Value (H₀: $b = 0$)	0.000	0.000	0.000	*0.000*	0.000	0.000	0.000	***0.000***	0.000	*0.001*
Lower C.I. (P=0.95)	0.048	0.792	0.808	*0.887*	0.048	0.174	0.309	***0.935***	1.062	*0.311*
Higher C.I. (P=0.95)	0.190	0.984	0.946	*1.075*	0.096	0.280	0.457	***1.115***	1.430	*1.177*
$I(d)/I_{max}(d)$ (0-500km)	0.036	-0.021	0.404	*0.598*	0.344	0.254	-0.271	***0.574***	0.605	*0.048*

	Supplementary Table 1i: All Quartiles - Range Scatter Models								
	Topographic surface area	NPP	Precipitation	Temperature	Topographic Relief	Ecosystem Diversity	Species Energy	Water Energy	Temperature Kinetics
Ordinary Regression									
r^2	0.196	0.439	0.390	0.250	0.004	0.064	0.463	0.330	0.243
P (n*)	0.004	0.002	0.005	0.036	0.647	0.013	0.002	0.018	0.042
$I(d)/I_{max}(d)$ (0-500km)	0.733	0.652	0.658	0.692	0.780	0.820	0.642	0.667	0.692
Spatial Regression Needed	Needed	Needed	Needed	Needed	Needed	Needed	Needed	Needed	Needed
Model	GLS	GLS	GLS	GLS	GLS	GLS	GLS	GLS	GLS
Intercept	97.601	74.689	92.064	137.315	40.729	35.949	101.028	122.670	291.227
P-Value (H$_0$: $a = 0$)	0.000	0.000	0.000	0.000	0.166	0.244	0.000	0.000	0.000
Lower C.I. (P=0.95)	57.268	41.925	38.741	96.017	-16.868	-24.017	74.327	82.315	191.471
Higher C.I. (P=0.95)	137.934	107.453	145.387	178.613	98.326	95.915	127.729	163.025	390.983
Slope	0.211	0.273	0.043	-0.166	0.214	0.285	0.241	-0.073	-1.113
P-Value (H$_0$: $b = 0$)	0.000	0.000	0.239	0.009	0.000	0.000	0.000	0.265	0.000
Lower C.I. (P=0.95)	0.148	0.186	-0.029	-0.290	0.196	0.253	0.187	-0.201	-1.652
Higher C.I. (P=0.95)	0.274	0.360	0.115	-0.042	0.232	0.317	0.295	0.055	-0.574
$I(d)/I_{max}(d)$ (0-500km)	0.021	0.095	0.010	0.083	0.254	0.140	0.037	0.083	0.229

	Supplementary Table 1j: All Quartiles - Range Cohesion Models									
	Topographic surface area	NPP	Precipitation	Temperature	Topographic Relief	Ecosystem Diversity	Species Energy	Water Energy	Temperature Kinetics	Geometric Constraints
Ordinary Regression										
r^2	0.271	0.437	0.423	0.343	0.018	0.119	0.426	0.385	*0.256*	0.162
P (n*)	0.026	0.006	0.008	0.011	0.473	0.111	0.008	0.013	*0.033*	0.088
$I(d)/I_{max}(d)$ (0-500km)	0.738	0.684	0.693	0.716	0.775	0.811	0.688	0.702	*0.748*	0.774
Spatial Regression	Needed	Needed	Needed	Needed	Needed	Needed	Needed	Needed	*Needed*	Needed
Model	GLS	GLS	GLS	SAR	GLS	GLS	SAR	SAR	*SAR*	GLS
Intercept	93.457	50.713	58.206	59.031	28.315	23.496	82.817	48.136	*-3.781*	-24.488
P-Value (H$_0$: a = 0)	0.000	0.001	0.000	0.003	0.360	0.420	0.000	0.013	*0.900*	0.448
Lower C.I. (P=0.95)	55.406	19.844	25.004	19.757	-32.338	-33.641	54.523	10.231	*-63.067*	-87.808
Higher C.I. (P=0.95)	131.508	81.582	91.408	98.305	88.968	80.633	111.111	86.041	*55.505*	38.832
Slope	0.337	0.634	0.532	0.512	0.294	0.508	0.492	0.613	*0.977*	1.192
P-Value (H$_0$: b = 0)	0.000	0.000	0.000	0.000	0.000	0.000	0.000	0.000	*0.000*	0.000
Lower C.I. (P=0.95)	0.233	0.501	0.404	0.319	0.266	0.452	0.400	0.422	*0.585*	0.792
Higher C.I. (P=0.95)	0.441	0.767	0.660	0.705	0.322	0.564	0.584	0.804	*1.369*	1.592
$I(d)/I_{max}(d)$ (0-500km)	-0.026	0.009	-0.032	-0.024	0.281	0.356	-0.002	-0.026	*0.000*	0.311

Supplementary Table 2. Explanatory factors for species richness of endemic birds of South America ($n = 2,248$). Tabled values are coefficients of determination (r^2) from simple (OLS), one-predictor regressions of observed species richness on raw environmental variables. Results are shown for species partitioned into range size quartiles, for the species of the first three quartiles pooled, and for all quartiles pooled. Shaded gray cells contain results for all climate models for species of the first three quartiles (smaller ranges). [A] denotes a negative regression slope. Supplementary table 4 shows the corresponding results for all breeding birds of South America ($n = 2,891$).

Quartile	First quartile	Second quartile	Third quartile	Quartiles (1 + 2 + 3)	Fourth quartile	All quartiles
Factor						
Precipitation (mm/yr^{-1})	0.00	0.00	0.02	0.01	0.43	0.35
Temperature (mean annual, °C)	0.01[A]	0.02[A]	0.02[A]	0.02[A]	0.47	0.25
Net primary productivity (tons carbon per hectare per year)	0.00[A]	0.00[A]	0.00	0.00[A]	0.64	0.44
Topographic surface area (km^2)	0.01	0.00	0.01	0.01	0.24	0.21
Ecosystem diversity (number of ecosystems in cell)	0.21	0.22	0.19	0.24	0.00 [A]	0.07
Topographic relief (elevational range, m a.s.l.)	0.34	0.42	0.22	0.36	0.19 [A]	0.00 [A]

Supplementary Table 3. Explanatory factors for species richness of all breeding birds of South America ($n = 2{,}891$). Tabled values are coefficients of determination (r^2) for predictors of species richness, generated by the Range Scatter model (RS) and the Range Cohesion model (RC) based on a simple (OLS) regression of observed on predicted species richness. Species were partitioned into range-size quartiles. Shaded gray cells contain results for all climate models for species of the first three quartiles (smaller ranges). [A]Denotes negative regression slope. The corresponding for endemic birds of South America ($n = 2{,}248$) are shown in Supplementary table 1.

Quartile	First quartile		Second quartile		Third quartile		Fourth quartile		All quartiles	
Factor	**RS**	**RC**	**RS**	**RC**	**RS**	**RC**	**RS**	**RC**	**RS**	**RC**
Precipitation (mm/yr^{-1})	0.01	0.00	0.01	0.00	0.08	0.03	0.67	0.80	0.60	0.62
Temperature (mean annual, °C)	0.00[A]	0.00[A]	0.00[A]	0.02[A]	0.00	0.00[A]	0.67	0.74	0.48	0.48
Net primary productivity (tons carbon per hectare per year)	0.00	0.00[A]	0.00[A]	0.01[A]	0.05	0.01	0.79	0.83	0.66	0.60
Topographic surface area (km^2)	0.00	0.00	0.00	0.00[A]	0.02	0.00	0.20	0.42	0.16	0.27
Ecosystem diversity (number of ecosystems in cell)	0.21	0.21	0.23	0.22	0.18	0.10	0.00	0.12	0.06	0.11
Topographic relief (elevational range, m a.s.l.)	0.31	0.29	0.38	0.35	0.16	0.11	0.17[A]	0.20[A]	0.02[A]	0.04[A]

Supplementary Table 4. Explanatory factors for species richness of all breeding birds of South America (n = 2,891). Tabled values are coefficients of determination (r^2) from simple (OLS), one-predictor linear regressions of observed species richness on raw environmental variables. Results are shown for species partitioned into range size quartiles, for the species of the first three quartiles pooled, and for all quartiles pooled. Shaded gray cells contain results for all climate models for species of the first three quartiles (smaller ranges). [A] denotes a negative regression slope. Supplementary table 2 shows the corresponding results for endemic birds of South America (n = 2,248).

Quartile	First quartile	Second quartile	Third quartile	Quartiles (1 + 2 + 3)	Fourth quartile	All quartiles
Factor						
Precipitation (mm/yr^{-1})	0.01	0.01	0.07	0.04	0.57	0.53
Temperature (mean annual, °C)	0.00[A]	0.00[A]	0.00	0.00[A]	0.69	0.48
Net primary productivity (tons carbon per hectare per year)	0.00[A]	0.00[A]	0.05	0.01	0.82	0.67
Topographic surface area (km^2)	0.00	0.00	0.02	0.00	0.24	0.21
Ecosystem diversity (number of ecosystems in cell)	0.21	0.23	0.19	0.25	0.00	0.07
Topographic relief (elevational range, m a.s.l.)	0.31	0.39	0.16	0.33	0.14[A]	0.00[A]